

# Macroporous chitosan/polyvinyl alcohol composite adsorbents based on activated carbon substrate

Ehsan Salehi<sup>1</sup> · Atefeh Farahani<sup>1</sup>

Published online: 10 January 2017  
© Springer Science+Business Media New York 2017

**Abstract** In current work, granular activated carbon (AC) was impregnated with different blends of chitosan (CS) and polyvinyl alcohol (PVA), (1:1, 1:2 and 2:1 w/w) polymers. Batch adsorption of methylene blue from water was studied using composite adsorbents. Isotherms and kinetics of adsorption on pristine, acidified and composite ACs were investigated and compared. FTIR, SEM, synthesis yield, swelling ratio and abrasion hardness analyses were selected for characterizing the adsorbents. Pseudo-first-order, pseudo-second-order and intraparticle diffusion models were employed to study the adsorption kinetics and, the pseudo-first-order model provided a better fit. Equilibrium results revealed that both Langmuir and Freundlich isotherms could well describe the adsorption equilibrium. Activated carbon/chitosan adsorbent suggested the highest adsorption capacity (468.7 mg/g) which was around 33 mg/g larger than that of the pristine activated carbon (435.2 mg/g). Moreover, AC/CS/PVA composites demonstrated the superior uptake rate and swelling degree in spite of having inferior yield of production. The hardness value was improved as a result of the polymer coating especially with the blends of CS and PVA due to developed interconnected network of the resultant coating layer. Generally, the results indicated that the role of CS was more highlighted in elevation of adsorption capacity while PVA was more effective in kinetic rate enhancement.

**Keywords** Composite adsorbents · Adsorption · Activated carbon · Chitosan · Polyvinyl alcohol.

✉ Ehsan Salehi  
ehsan1salehi@gmail.com; e-salehi@araku.ac.ir

<sup>1</sup> Department of Chemical Engineering, Faculty of Engineering, Arak University, Arak 38156-8-8349, Iran

## 1 Introduction

Nowadays, water resources are in growing risk of industrial contamination. Dyes and pigments are among the most important contaminants due to their widespread generation and application. Many types of dyes are used and/or produced in food, textile, beverage and cosmetics industries. In addition to ecosystem infection, these pollutants can cause different types of diseases for animals and human beings because of their carcinogenicity and toxicity [1]. Methylene blue is one of the most common dyes used in the textile industries. Many techniques have been investigated to remove methylene blue and other similar dyes from aqueous environment. Adsorption, coagulation, precipitation, advanced oxidation, membrane filtration and ion exchange are common examples of these techniques [2]. In addition, some researchers have combined two or more of these techniques to obtain more effective and environment-friendly removal procedures [3]. One of the most popular processes for this purpose is adsorption. Simplicity of design, ease of control, economic appropriateness, reusability, preferable selectivity, secondary wastes minimization and ease of scale up are some advantages of the adsorption processes.

In the area of water and wastewater treatment, a great deal of researches has concentrated on activated carbons (ACs) as the well-established and most effective adsorbents [4, 5]. High surface area, developed micro/meso porous structure, acceptable mechanical/chemical stability, adsorption capacity and affordable economy are obvious advantages of activated carbon adsorption [6]. Activated carbons from agricultural waste/by-product sources are usually biocompatible, biodegradable, and particularly, interesting from economical viewpoint. Pristine (without any treatment) activated carbon is not always favorably effective for the elimination of pollutants from aqueous phase

especially in low (trace) concentrations. In addition, physicochemical properties of ACs like abrasion hardness and mechanical stability should be improved for some specific applications. Accordingly, a lot of modification techniques have been developed in order to enhance ACs properties. Plasma treatment, chemical deposition, acid/base treatment, impregnation, ozone treatment, microwave irradiation and preparation of carbon/modifier(s) composites are some of the techniques addressed in the literature [7, 8].

Biomodifiers like chitosan have recently attracted researchers' attention for their availability and biocompatibility. Chitosan (CS) is a natural amino-polysaccharide biopolymer. Polymer chains of chitosan contain abundant amino and hydroxyl functional groups as strong reactive sites for adsorption of macromolecules, dyes and heavy metal ions. This polymer is also biocompatible, biodegradable, non-toxic and available in low cost [9]. These properties encourage researchers and industrials to apply CS and CS composites for water and wastewater treatment as well as biological separations. Moreover, CS has been applied for the preparation of different materials being applied in bioengineering such as hydro-gels, membranes, beads and composite adsorbents. In spite of many advantages, CS and CS derivatives possess some undesirable characteristics such as relative dissolution in acidic media, insufficient mechanical resistance and possibility of chemical degradation [10]. Most of these problems can be overcome by blending CS with appropriate copolymers including polyether sulfone [11], polylactic acid [12], polyether block amine [13], polyethylene glycol [14], and polyvinyl alcohol (PVA) [15, 16]. Current authors have selected and applied PVA as a potential blending agent for CS to prepare composite CS/PVA membrane adsorbents with improved stability and adsorption performance [16]. Enhanced properties of CS/PVA blends are ascribed to the interactions and interconnections between CS and PVA polymer chains i.e., hydrophobic interactions, aggregation, ether connections and intermolecular/intramolecular bonding. Providing required mechanical stability, increasing the reactivity of the resultant composite by introducing additional hydroxyl functional groups and generating pores in CS polymer background as a result of the difference in solubility with CS, are other advantages of PVA as blending agent for chitosan.

Some researchers have applied CS or PVA separately to modify activated carbons [10, 17–19]. AC/CS composites have been successfully used for the adsorption of anionic and cationic dyes by Auta et al. [10]. Maghsoodloo et al. [17] investigated the CS treated activated carbon for the effective removal of humic acid. The amino groups of CS are highly reactive sites for the adsorption of negatively charged species from aqueous phase. A comparative study on CS, AC and AC/CS composites

has been done for cadmium adsorption from water [18]. Results revealed that the adsorption capacity of the AC/CS composite is much more than the other applied adsorbents [18]. PVA/AC composites have been fabricated by Sandeman et al. [19] to remove anionic and cationic dyes from water in dynamic adsorption mode i.e., packed bed columns. Results emphasized the important role of PVA in enhancement of mechanical stability of activated carbon.

To our knowledge, application of CS/PVA blend for the preparation of activated carbon/polymer composites has not been addressed elsewhere. In the current study, walnut shell-based granular AC was modified with CS/PVA polymer blends with different CS to PVA weight ratios. Batch adsorption tests were conducted to evaluate the properties of these novel composite adsorbents for methylene blue removal from water. SEM, FTIR, swelling, yield and hardness analyses were employed to characterize the morphological, chemical, mechanical and economical properties of the prepared adsorbents.

## 2 Experimental details

### 2.1 Materials

Walnut-shell based, physically activated granular activated carbons were gifted by Part Chemical Company, Iran. The specifications of the activated carbons are summarized in Table 1. Fully hydrolyzed polyvinyl alcohol (MW = 60,000) and methylene blue were purchased from Merck (Germany). Chitosan polymer (MW = 100,000–300,000) with 90% degree of deacetylation was obtained from Acros (USA). Oxalic acid, NaOH and HCl were of analytical grades. Double-distilled water was used during all the experiments.

**Table 1** Specifications of pristine activated carbon

Activated carbon property	Quantity
Type	Granular
Mesh (US standard sieve size)	8×30
Precursor	Walnut hard shell
Iodine number (mg/g)	1200±10
BET (m <sup>2</sup> /g)	1240–1300
Bulk density (kg/m <sup>3</sup> )	300±10
pH	10–11
Ash content (max. %)	7
Moisture content (max. %)	5

## 2.2 Preparation of adsorbents

To prepare different adsorbents, firstly, 120 g of AC was poured in oxalic acid (0.2 M). After 4 h rest, the solution was filtered and the acidified AC was collected, washed with double-distilled water and dried in the oven at 70 °C overnight. The acidified AC was used to prepare subsequent adsorbents.

AC/CS composite (ACC) was synthesized by adding 2.5 g of CS into 250 ml of 0.2 M oxalic acid solution under rigorous stirring (1000 rpm) at 50 °C. After 1.5 h a light yellow gel was obtained. Then, 20 g of the acidified AC was gradually added to the CS gel and stirred (750 rpm) for 16 h at 50 °C. The AC/CS mixed gel was poured into 0.5 M NaOH bath to normalize the pH and stabilize the coating layer on the AC. After 45 min the adsorbents were filtered, washed several times and dried in an oven at 70 °C. AC/PVA composites were prepared by adding 20 g of the AC into the PVA solution prepared by dissolving 2.5 g of PVA in 250 ml oxalic acid (0.2 M). Subsequent steps are similar to the AC/CS preparation steps.

To produce binary-polymer modified adsorbents, AC/CS/PVA, namely ACCP, with equal polymer to AC weight ratios, i.e. CS/AC = PVA/AC (W/W) (named as ACCP 1:1), the following procedure was followed. Firstly, 2.5 g of PVA was added to 125 ml of hot water (100 °C) and stirred for 1.5 h. Then, the solution was mixed with the CS gel prepared by dissolving 2.5 g of CS in 125 ml of 0.4 M oxalic acid solution. After 1.5 h, 20 g of the acid treated AC was gradually entered into the CS/PVA solution and stirred continuously for 16 h at 50 °C. After that, the adsorbents were filtered and soaked in 0.5 M NaOH solution bath. Finally, the composite adsorbents were filtered, washed and oven-dried as before. For the preparation of two other CS/PVA blends, 2:1 and 1:2 (W/W), just different amounts of PVA to CS were used and the other conditions were the same. Hereafter, ACCP (x:y) represents the activated carbon impregnated by an x (chitosan) to y (polyvinyl alcohol) weight ratio blend.

## 2.3 Characterization

### 2.3.1 SEM

Scanning electron microscope (Philips-X130 and Cambridge SEM, USA) was applied to study the microstructure morphology of the adsorbents.

### 2.3.2 Abrasion

The chemical resistance of the composite adsorbents against attrition was compared with each other according to the abrasion hardness analysis. The analysis procedure

was designed to measure the chemical stability of the composites against attrition. Precise amount of adsorbent was encountered with standard solution of acetate buffer for a specific period of time. Adsorbent was then weighted again after being washed with distilled water, and air-dried. The difference between the initial and final weight of the sample gives an estimate of its resistance against physicochemical attrition. Accordingly, abrasion hardness is defined by the following equation:

$$\%H = \frac{W_i - W_f}{W_i} \times 100 \quad (1)$$

where  $W_i$  and  $W_f$  are the initial and final mass of the adsorbent sample, respectively.

### 2.3.3 FTIR

Fourier transform infrared (FTIR) test was performed to identify the functional groups attached to the adsorbents before and after modifications as well as to understand the successfulness of the impregnation process. ABB Bomem (model: MB-104) FTIR spectrometer was used for this purpose.

### 2.3.4 Swelling ratio

An exact amount of adsorbent sample was kept in the distilled water at the ambient temperature overnight. The swelling ratio is defined by the following equation:

$$SR(\%) = \frac{W_w - W_d}{W_d} \times 100 \quad (2)$$

where  $W_w$ ,  $W_d$  are the wet and dried mass of the adsorbent sample, respectively. All the tests were conducted twice and the average values were reported.

## 2.4 Kinetics

The adsorbed amounts during batch adsorption tests were measured at different times to study the kinetics of the adsorption. In each test, 0.1 g of an adsorbent was placed in a 200 ml Erlenmeyer flask containing 100 ml of the methylene blue solution. The mixtures were agitated at 50 °C under 250 rpm for 7 h. During the operation, the concentration of the methylene blue solutions was monitored vs time using a UV-spectrophotometer at a wavelength of 665 nm. The adsorption capacity was calculated by the following equation:

$$q_t = \frac{(C_0 - C_t)V}{m} \quad (3)$$

where  $q_t$  is the amount of the solute adsorbed per unit mass of the adsorbent (mg/g),  $C_0$  and  $C_t$  are the initial and

time-dependent concentrations of MB (mg/L), respectively, and  $V$  (L) is the volume of the MB sample solution.

In order to understand the kinetics and mechanism of the adsorption reaction, pseudo-first order, pseudo-second order and intra-particle diffusion models were employed.

The linear form of the pseudo-first-order model is:

$$\log(q_e - q_t) = \log q_e - \frac{k_1 t}{2.303} \quad (4)$$

where  $k_1$  ( $\text{min}^{-1}$ ) is the rate constant of the pseudo-first-order model and can be obtained by plotting the logarithm of  $(q_e - q_t)$  versus time.  $q_e$  and  $q_t$  are the amounts of the solute adsorbed per unit mass of the adsorbent (mg/g) at equilibrium and at time  $t$ , respectively.

The pseudo-second-order model equation is as follows:

$$\frac{t}{q_t} = \frac{1}{k_2 \cdot q_e^2} + \frac{t}{q_e} \quad (5)$$

$k_2$  (mg/g min) is the pseudo-second-order rate constant.  $k_2$  and  $q_e$  can be obtained from the intercept and slope of the  $\frac{t}{q_t}$

versus  $t$  plot.

The intra-particle diffusion model is also given as:

$$q_t = K_{id} t^{0.5} \quad (6)$$

The slope of the  $q_t$  versus  $t^{0.5}$  plot is  $K_{id}$  (mg/g  $\text{min}^{1/2}$ ), the rate constant of the model.

## 2.5 Equilibrium

Equilibrium experiments were conducted in batch mode by equilibrating 0.1 g of an adsorbent in 100 ml of the MB solutions with different initial concentrations (50–1000 mg/l) at a fixed pH of 6.0. The solution samples were stirred at the room temperature under 250 rpm for 24 h. Final concentration of MB solutions was determined by a UV-spectrophotometer at 665 nm. The amount of the methylene blue adsorbed per unit mass of the adsorbent ( $q_e$ ) can be calculated by:

$$q_e = \frac{(C_0 - C_e)V}{m} \quad (7)$$

where  $C_e$  is the equilibrium concentration of MB in supernatant (mg/l).

The obtained experimental equilibrium data were fitted to the Langmuir and Freundlich isotherms. The non-linear equation defining the Langmuir isotherm is:

$$q_e = \frac{q_{\max} k_L C_e}{1 + k_L C_e} \quad (8)$$

where  $q_{\max}$  and  $k_L$  are the adsorption capacity of the adsorbent (mg/g) and the Langmuir constant (l/mg), ascribed to the energy of adsorption. To identify how favorable is

the adsorption process, separation factor ( $R_L$ ) was applied. The adsorption process is favorable if for the value of  $R_L$  defined by the following equation, we have  $0 < R_L < 1$ .

$$R_L = \frac{1}{1 + k_L C_0} \quad (9)$$

The Freundlich isotherm equation can be also written as:

$$q_e = k_f \cdot C_e^{1/n} \quad (10)$$

where  $k_f$  ( $\text{mg}^{1-1/n} \text{l}^{1/n}$ ) is the Freundlich constant, which is related to the adsorption rate, and the ratio  $1/n$  is related to the intensity of adsorption.

## 3 Results and discussion

### 3.1 Characterization

#### 3.1.1 FTIR

The FTIR spectra of the adsorbents, within the range of 500–4000  $\text{cm}^{-1}$  wavenumber, are shown in Fig. 1. In the FTIR spectra for AC (A), the adsorption band around 3300–3500  $\text{cm}^{-1}$  is attributed to the stretching vibration of the O–H groups. The weak peaks at 2800  $\text{cm}^{-1}$  are related to the C–H bonds of aliphatic and carboxylic groups, and also can present methyl and methylene vibrations. In addition, the peaks at 1300–1700  $\text{cm}^{-1}$  region indicate the existence of C=O in carbonyl and aromatic groups on the AC [18, 20]. Increasing the number of the peaks at 3300–3800  $\text{cm}^{-1}$  region in FTIR spectra of the acidified AC (B) indicates the successfulness of the acidification process. For ACC (C), where AC is coated by chitosan, the adsorption band around 3300–3700  $\text{cm}^{-1}$  is attributed to the stretching vibration of O–H and extension vibration of N–H bonds of primary amine of chitosan. Moreover, peaks at 1630  $\text{cm}^{-1}$  show the N–H bending vibrations of the  $\text{NH}_2$  group belonging to chitosan polymer [10, 18]. In FTIR spectra of ACP (D), peaks at 3133–3674  $\text{cm}^{-1}$  are attributed to the stretching vibration of O–H, the most abundant functional groups available in PVA. So, by comparing this spectrum with the FTIR spectra of the AC, it is revealed that the PVA polymer has been successfully coated on the AC [21].

In the FTIR spectra of ACCP (E), the thickness of the peaks at 3200–3570  $\text{cm}^{-1}$  region shows the N–H vibration of chitosan and O–H vibration in both chitosan and PVA. The adsorption band around 1640  $\text{cm}^{-1}$  is related to the  $\text{NH}_2$  vibrations of chitosan. Thus, for all the adsorbents, the FTIR spectra confirm the appropriateness of the impregnation processes.

**Fig. 1** FTIR spectra of adsorbents :AC (a), Acidified AC (b), ACC (c), ACP (d), ACCP (e)

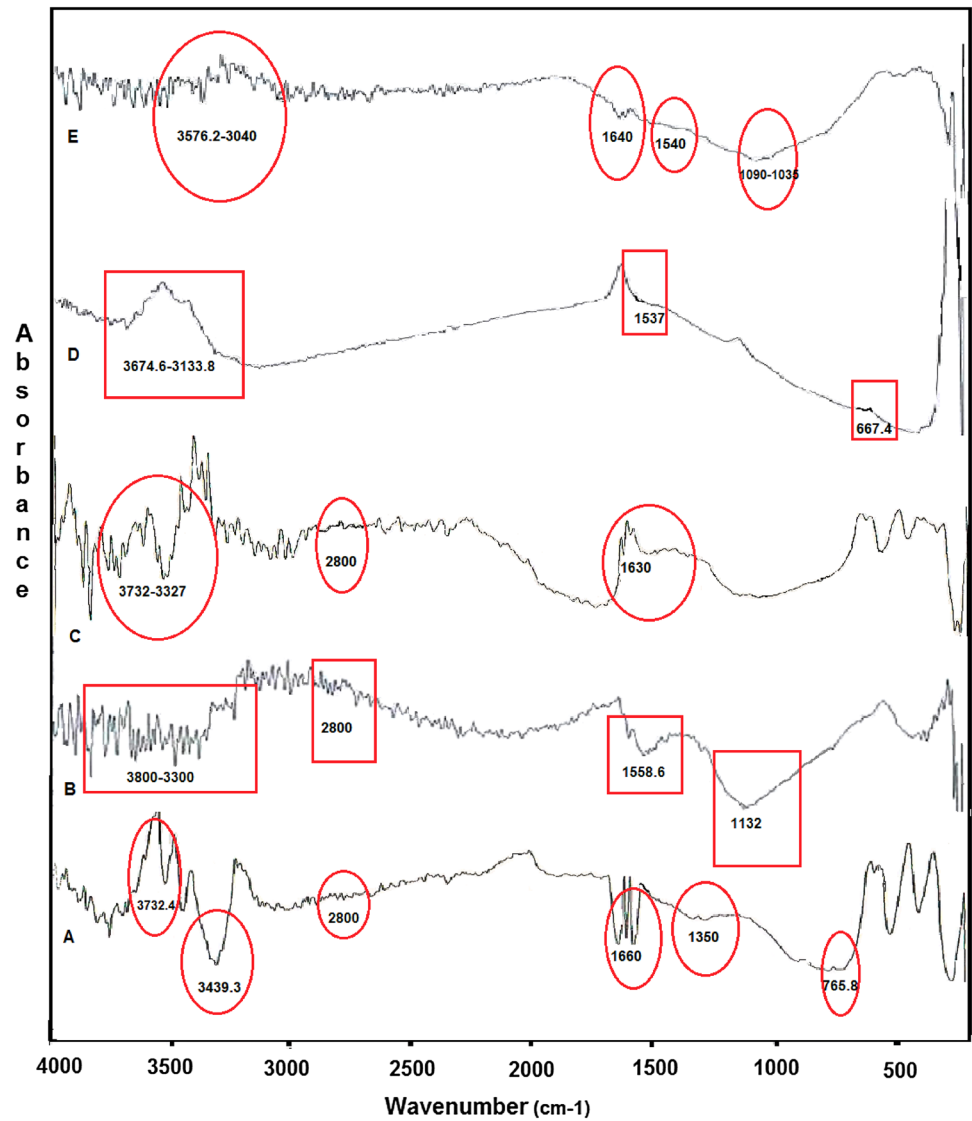


**Table 2** Abrasion hardness (*H*) and synthesizing yield for different adsorbents

Adsorbent	%H	Yield
AC	85.3	–
AAC	83.2	–
ACC	87.2	0.80
ACP	90.3	0.84
ACCP1:1	90.7	0.57
ACCP2:1	92.3	0.50
ACCP1:2	90.7	0.68

3.1.2 Abrasion hardness

Table 2 shows the results of the abrasion hardness analysis for the pristine and modified activated carbons. According

to the results, the polymer impregnation could improve the hardness of the activated carbons.

Abrasion resistance demonstrates the physicochemical stability of the composite adsorbents. PVA has been used by other researchers to increase the mechanical stability of composite materials [21]. This polymer has been employed for two important purposes; crosslinking and providing a blending agent [16]. In addition, the results depicted in Table 2 confirm that PVA has a pivotal effect on the hardness improvement. A comparison between CS and PVA was performed to understand which of the polymers has a higher thermochemical resistance. In the same condition, that is the same stirring rate, temperature, pH and concentration, the time required for the complete dissolution of PVA in oxalic acid (0.2 M) solution was more than that of chitosan. This observation revealed that PVA has higher

thermochemical stability. Based on the results, CS has also positive effect on the hardness of the ACC composites. It was probably occurred because of the reaction between the amine groups of CS and carbonyl and carboxyl groups available on the AC surface. This is the so-called Schiff base reaction and provides the favorable condition for the appropriate stabilization of the polymer networks on the activated carbon surface.

The activated carbons impregnated with the blends of CS and PVA tabulated higher hardness amounts. Strong interactions/interconnections between the functional groups of the two polymers through intermolecular hydrogen bonding, bridging ether connections and aggregation are responsible for this observation. Figure 2 schematically illustrates some of these interactions.

Accordingly, an inter-connected (crosslinked) binary polymer network forms and covers the surface of the activated carbon. This coating layer can protect the AC against abrasion. The composite coating layer can be appropriately immobilized on the AC surface by the Schiff base reaction, as shown in Fig. 3.

### 3.1.3 SEM

Figures 4 and 5 show SEM micrographs of AC, ACC, ACP and ACCP with different magnifications.

The average size of the pores and pore-wall thickness can be estimated through the images. Figures 4a and 5a show the SEM images of the pristine AC before the acidification process. At the left corner of the image 4(A), an undeveloped porous structure with a lot of interstices can be seen. These interstices might be stacks of randomly crosslinked aromatic sheets and appeared as a result of imperfect carbonization process. Although after activation process, most of the carbonaceous materials would be activated, the performance of the activation process highly depends on the nature of raw material used, activating agent and the operating conditions [23].

Figures 4b and 5b indicate the microstructure of the ACC. It is obvious that the average pore-wall thickness is higher than that of the other composites. The reason may be related to the well immobilization of CS chains on the AC surface through the Schiff base reactions between carbonyl groups of AC and amine group of CS. The number and average size of the opened pores is larger in the ACP

**Fig. 2** Interactions between CS and PVA polymeric chains

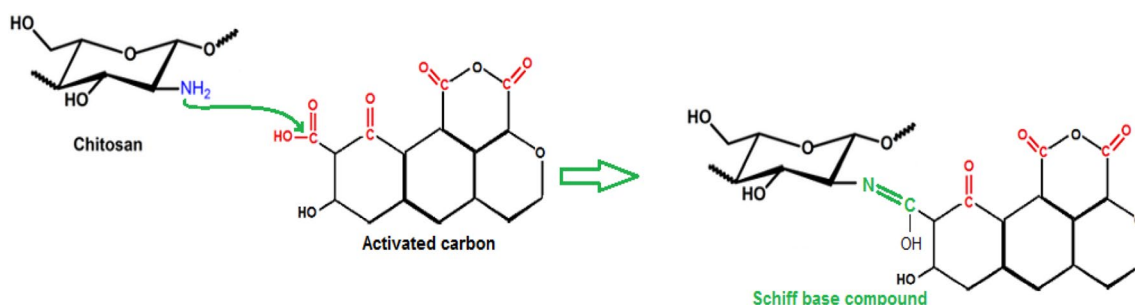
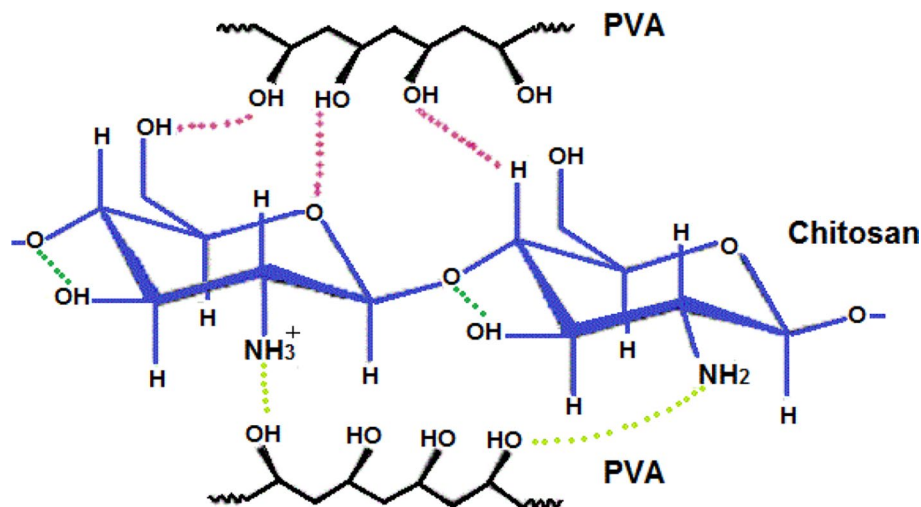


**Fig. 3** Schiff-base reactions between AC and CS functional groups

**Fig. 4** SEM images of AC (a), ACC (b), ACP (c), and ACCP (d)

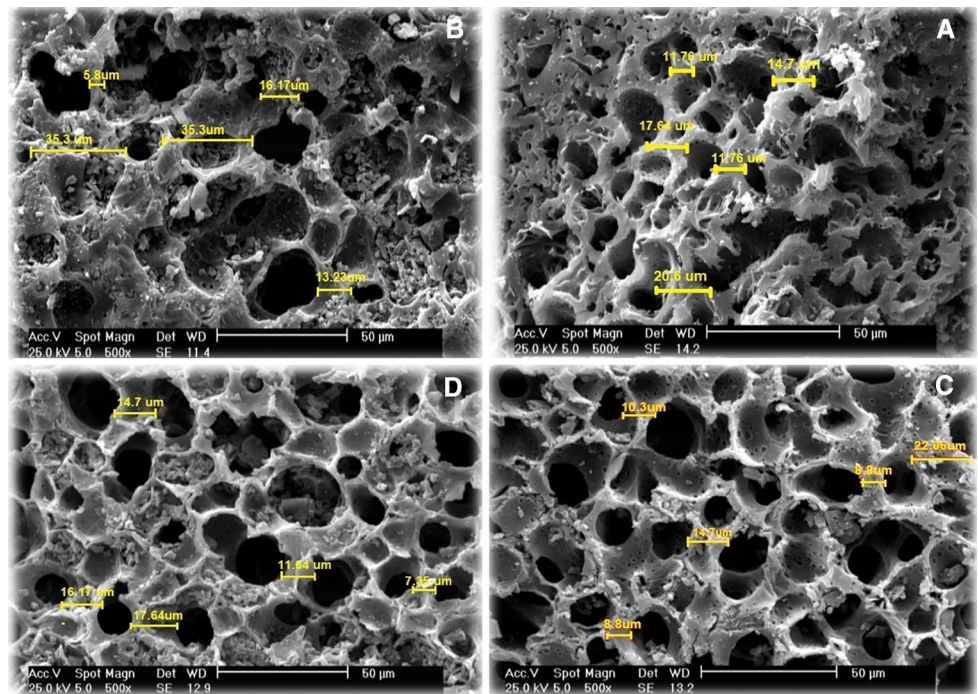
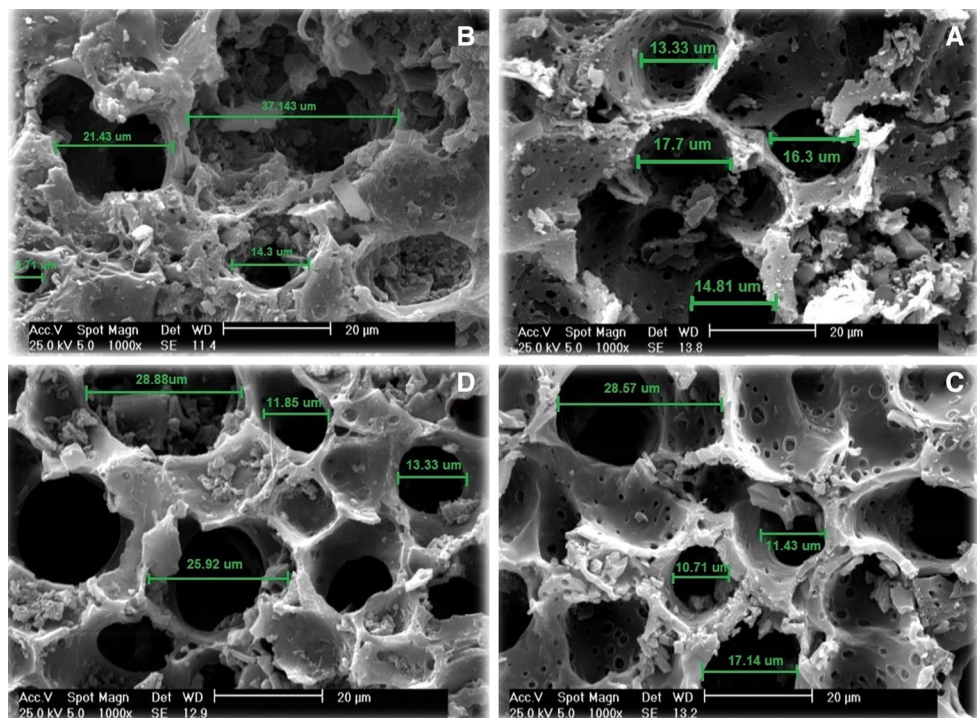


**Fig. 5** SEM images of AC (a), ACC (b), ACP (c), and ACCP (d)



composite (Figs. 4c, 5c). It is inferred from the results that the PVA chains are not attached to the AC surface as favorably as the CS chains. In the preparation step, PVA dissolves much easier than CS in the alkaline bath. Therefore, the coating layer thickness in the ACC structure is larger than that of the ACP. Figures 4d and 5d exhibit

micrographs of ACCP composite. The number of the open pores falls between that of the ACC and the ACP. Selective dissolution of PVA from the CS/PVA blend coating into the alkaline bath is responsible for the increased number of the open pores compared to the ACC. On the other hand, the interconnection of CS and PVA chains reduces

the dissolution rate of PVA into the alkaline solution during the fabrication. This is the reason for the decreased number of the open pores relative to that of the ACP composite. For the ACCP and ACP the sphericity of the pores is higher comparing to other adsorbents. Moreover, the pores are more homogeneously distributed in the structure. This may be related to the influence of polyvinyl alcohol polymer. The density of the –OH groups highly increases with the addition of PVA polymer. Hydroxyl groups can accelerate the proton exchange mechanism during the phase inversion in alkaline solution. Presumably, this mechanism controls and homogenizes the selective dissolution mechanism responsible for the formation of the pores. The homogeneity of the distribution of the pores may be enhanced accordingly.

The order of the average thickness of the pore-wall of the different composites is as the following:

$$\text{ACC} > \text{AC} > \text{ACCP} > \text{ACP}.$$

The highest wall thickness is for the ACC. This is in agreement with the better stabilization of the CS chains on the AC surface as discussed before. The wall thickness of the ACCP is larger than that of the ACP. During the preparation process, the PVA solubility in the alkaline bath is higher than that of the CS. Moreover, the PVA/CS composite is better saved as the coating layer due to the favorable interconnections between the two polymer chains. The rank of the pristine AC in this tabulation is somewhat strange because it must tabulate the lowest wall thickness. In Fig. 5a, brilliant species are obvious in the image. These species are the ash particulates remained after the carbonization step. After the acid wash process, the carbonization ash and the other particulates of the decomposition leave the pores.

### 3.1.4 Swelling

The swelling ratio (SR%) of the adsorbents is in tune with their hydrophilicity. This property has a crucial effect on the adsorption behavior. Porosity and chemical functionality are two important affecting factors for the determination of the swelling ratio. According to the results (Fig. 6), although both of the polymers are hydrophilic, a small decrease in SR of ACC composite is observed when it is compared to AC and AAC.

This may be caused as a result of the deacetylation of the chitosan [24] as well as the reduction of the activated carbon porosity due to pore blockage by this polymer (as obvious in SEM images). The decrease in the value of SR for the ACP presumably originates from selective dissolution of PVA in NaOH solution during preparation. Thus, a large number of hydrophilic hydroxyl groups in the PVA structure might be lost. The ACCP composites demonstrated a higher swelling ratio comparatively. This may be attributed

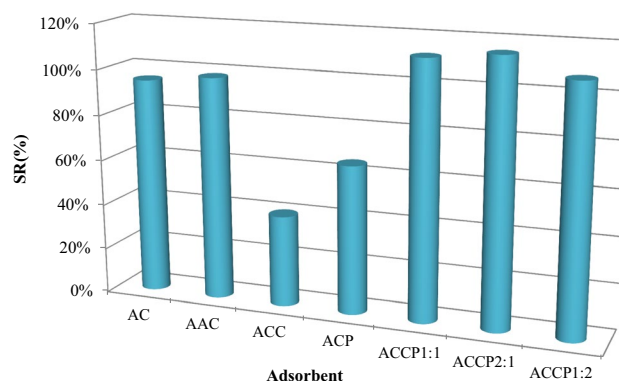


**Fig. 6** Swelling ratio of different adsorbents

to the interconnected porous network of the CS/PVA coating layer with abundant hydrophilic –OH and –NH<sub>2</sub> functional groups [16].

### 3.1.5 Synthesis yield

Yield of production is an important factor especially from economical point of view. Unfortunately, recent researches pay no sufficient attention to this important issue which sometimes challenges the feasibility of the process for the scale up and full scale implementation.

Yield of synthesis can be estimated from the following equation:

$$\text{yield} = \frac{W_f}{W_i + W_p} \quad (11)$$

where  $W_f$  is the final mass of the synthesized adsorbent,  $W_i$  is the mass of the pristine activated carbon used and  $W_p$  is the total mass of the applied polymers. Yields of production for different adsorbents are depicted in Table 2. Yield is always less than 100% because a portion of activated carbon and/or polymer modifiers may be dissolved in oxalic acid and/or alkaline solution during the modification process and lost. In addition, the activated carbon composites with pure polymer coating (ACC and ACP) offer higher yield of production comparing to the binary-polymer impregnated composites (ACCPs). This fact reveals that some part of the polymers has been dissolved in NaOH solution and lost. Furthermore, in ACCPs, some part of the functional groups of CS and PVA are participated in the interconnection-forming (crosslinking) reactions. Therefore, carbonyl groups of AC have a lower chance to strongly react with the functional groups of the mixed-matrix coating through the Schiff base reactions. Accordingly, the binary coating films are at a higher risk of dissolution during the modification process comparing to the pure polymer films.



As discussed in the previous section, the swelling ratio of the ACCP adsorbents was higher. There is an inverse relation between SR and Yield. The higher the swelling content, the fewer the production yield [25]. Moreover, composites with a superior water affinity are at a higher risk of dissolution in acidic media.

### 3.2 Kinetics

Kinetic study shows the effect of contact time on the methylene blue adsorption by different adsorbents. Adsorption increases sharply at the first part of the process and afterwards slows down to meet the equilibrium. The pseudo-first-order, pseudo-second-order and intraparticle diffusion (Webber-Morris model) kinetic models were used to test the experimental kinetic data and find out the mechanism of the adsorption. Kinetic parameters and regression coefficients ( $R^2$ ) for the pseudo-first and pseudo-second-order kinetic models are presented in Table 3.

Although, intraparticle diffusion model exhibits relatively acceptable correlation coefficient for different adsorbents, the  $q_t$  versus  $t^{0.5}$  lines do not pass through the origin. Hence, the intraparticle diffusion cannot be the rate controlling step.

Relatively high values of correlation coefficients ( $R^2 > 0.93$ ) were obtained for both of the pseudo-first-order and pseudo-second-order models. However, the agreement between the model-predicted  $q_e$  and experimental  $q_e$  was stronger for the pseudo-first-order model. Therefore, the pseudo-first order model is the model of choice. It can be understood that the adsorption is rather physical and proceeds by diffusion through the boundary layer.

Methylene blue is a cationic dye and positively charged in neutral pH. MB molecules can be adsorbed on to the negatively charged functional groups of the adsorbents i.e., carbonyl, carboxyl, hydroxyl and amino groups through physical interactions like electrostatic forces. Consequently, the ACCP (1:2), the acidified AC and the ACCP (1:1) with abundant protonated –OH groups tabulated higher uptake rate constants ( $k_1$ ), respectively.

### 3.3 Isotherms

Equilibrium adsorption data were fitted to the Langmuir and Freundlich adsorption isotherms. Isotherm constant parameters and regression coefficients are presented in Table 4.

Separation factor ( $R_L$ ) was also calculated for all the adsorbents at the initial concentration, 100 mg/l, and the

**Table 3** The parameters of pseudo-first-order and pseudo-second-order kinetic models

Adsorbent	Exp. $q_e$ (mg/g)	Pseudo-first-order model			Pseudo-second-order model		
		Model-calc. $q_e$	$K_1$ ( $h^{-1}$ )	$R^2$	Model-calc. $q_e$	$K_2$ ( $mg\ g^{-1}\ h^{-1}$ )	$R^2$
AC	66.38	58.58	0.198	0.95	75.17	0.0041	0.996
AAC	111.18	108.21	0.252	0.98	126.58	0.0024	0.999
ACC	56.98	57.016	0.198	0.98	64.4	0.00318	0.997
ACP	46.78	50.46	0.107	0.98	65.3	0.0017	0.967
ACCP1:1	20.78	22.376	0.245	0.93	30.3	0.00288	0.948
ACCP2:1	53.18	53.579	0.167	0.94	64.93	0.00273	0.963
ACCP1:2	23.78	25.34	0.412	0.98	25.57	0.0225	0.992

The number of data points for kinetic plots is 8

**Table 4** Constants and regression coefficients of Langmuir and Freundlich isotherms for different adsorbents

Adsorbents	Langmuir model				Freundlich model		
	$q_{max}$ (mg/g)	$K_L$	$R_L$	$R^{2a}$	$K_f$	$n$	$R^2$
AC	435.2	0.0038	0.72464	0.99	4.263	1.41	0.99
AAC	439.2	0.0051	0.66225	0.96	5.78	1.46	0.99
ACC	468.7	0.0031	0.76336	0.98	3.18	1.33	0.98
ACP	417.4	0.0033	0.75188	0.99	3.102	1.33	0.98
ACCP (1:1)	403.4	0.0032	0.75758	0.99	5.04	1.49	0.99
ACCP (2:1)	409.1	0.004	0.71429	0.95	4.69	1.45	0.96
ACCP (1:2)	400.3	0.0039	0.71942	1	4.9	1.49	0.99

The number of data points for isotherm plots is 10

<sup>a</sup>The maximum deviation of the model calculated values from the experimental data points was less than 5%

corresponding values were less than 1. This fact confirms the favorability of the adsorption process.

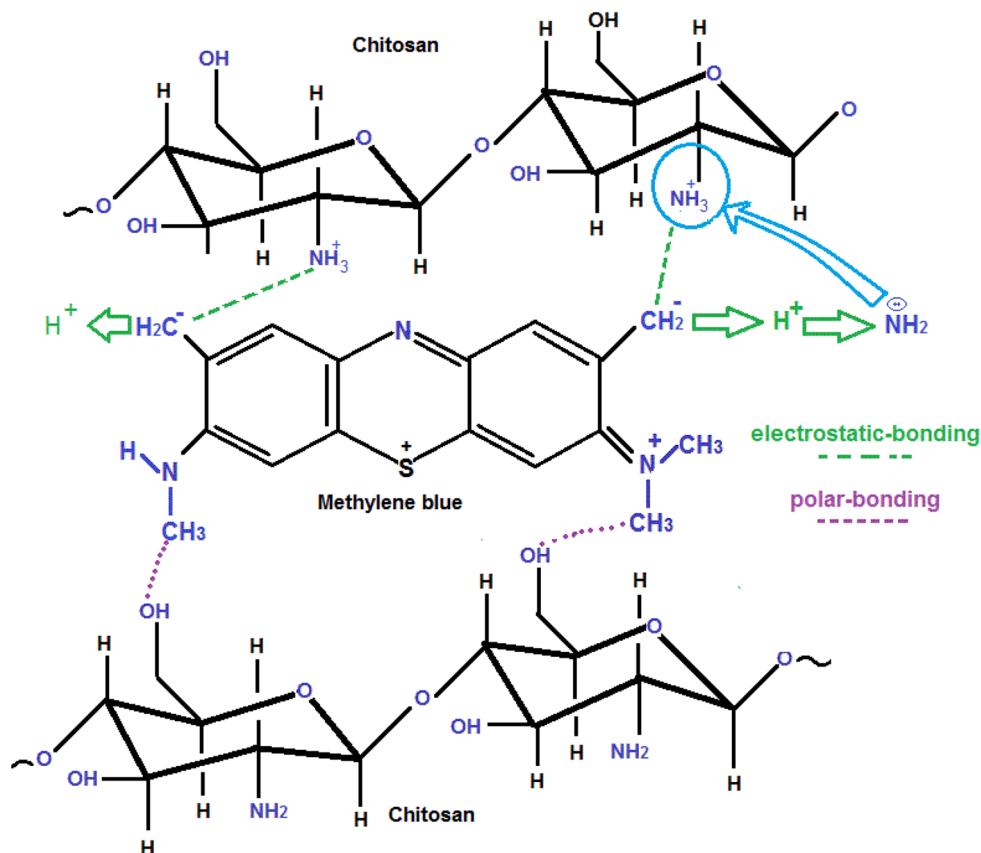
According to the results, both of the models are in good agreement with the experimental equilibrium data. Furthermore, the results showed that the ACC records the highest adsorption capacity among all the composites. Acidified AC, pristine AC and ACP recorded subsequent places, respectively. As mentioned in the previous sections, chitosan blocks a large number of pores and consequently, reduces the pore capacity and water affinity of the activated carbon. Thus, the adsorption capacity of ACC can be directly ascribed to the chemistry and reactivity of the functional groups of chitosan. Two important factors determine the adsorption capacity of an adsorbent i.e., the specific surface area and the chemistry. The first factor depends on the morphology and porosity of the adsorbent. The latter however, is in close relation to the reactivity and density of the functional sites available on the adsorbent surface. Impregnation by chitosan decreases the surface area by blocking a portion of the pores; however, it introduces a large number of reactive functional sites ( $-\text{OH}$  and  $-\text{NH}_2$ ) to the adsorbent surface. The latter effect seems to be more effective in determining the adsorption capacity when chitosan applied as the modifier. Methylene blue molecules can interact with the chitosan functional groups through covalence, electrostatic and hydrogen bonding. Figure 7

illustrates a schematic of the possible interactions between the chitosan and methylene blue molecules.

In ACP, the density and reactivity of PVA functional groups are not as large as CS; however, majority of the pores remains open. Thus, the adsorption capacity of ACP is smaller than that of ACC. In the ACCP adsorbents, adsorption capacity is further reduced compared to the other adsorbents. It is due to decreased number of the free functional sites and consequently, the slightly reduced reactivity of the polymers. Reducing the sharpness of the functional peaks in the FTIR spectra of ACCP comparing to the adsorbents modified with a single polymer confirms this conclusion. A large number of the functional groups are involved in side interconnection formation reactions and lost for the adsorption of MB. As a result, the adsorption capacity of the ACCP composites decreases. Generally, the crosslinking density has a reverse impact on the adsorption capacity as reported in the literature [26].

Selection of the suitable adsorbent highly depends on the process requirements. For example, single polymer-modified adsorbents (ACC, ACP) are of choice under the condition that the adsorption capacity is the most important concern for industrials. From another point of view, hardness is of more importance in some applications, especially in flow adsorption mode and thus, binary-polymer modified activated carbons (ACCPs) are preferable. Rate of adsorption

**Fig. 7** Methylene blue and Chitosan interactions



can be another key factor affecting the selection results. The time required for the saturation is in direct connection with the size of the equipment required in dynamic adsorption mode. Binary-polymer modified activated carbons (ACCPs) can provide better adsorption rates, compared to the single-polymer modified ACs. In summary, decision makers should optimize all of the mentioned parameters together with the most important economic considerations to attain the optimum selection.

#### 4 Conclusions

Composite polymer/activated carbon adsorbents with different CS to PVA ratios (0:0, 1:0, 0:1, 1:1, 1:2, 2:1) were synthesized in this work. Batch adsorption of methylene blue from aqueous solutions was investigated using the adsorbents. FTIR and SEM analyses results demonstrated functional groups and pore structure of the composites as well as successful coating of the polymers on the AC. Abrasion hardness results confirmed that interconnection of the CS and PVA molecules could play an important role in improving the physicochemical stability of the adsorbents. The adsorption kinetics was well represented by the pseudo-first-order model with a higher adsorption rate observed in the case of the ACCP adsorbents (0.167 to 0.412 h<sup>-1</sup>). Langmuir and Freundlich isotherms were well fitted to the equilibrium experimental data. Chitosan impregnated activated carbon recorded the highest adsorption capacity (468.7 mg/g) mainly because of the reactivity of the CS functional sites in interaction with the methylene blue molecules. The adsorption process for all the adsorbents was favorable. Composite activated carbons with single polymer coating showed a larger yield of production (around 80%) comparatively. Generally, composite AC/CS/PVA adsorbents suggest appropriate physical and chemical properties for the water treatment.

#### References

1. J. Georgin, G.L. Dotto, M.A. Mazutti, E.L. Foletto, J. Environ. Chem. Eng. **4**, 266–275 (2016)
2. J. Chang, J. Ma, Q. Ma, D. Zhang, N. Qiao, M. Hu, H. Ma, Appl. Clay. Sci. **119**, 132–140 (2015)
3. H.P. Carvalho, J. Huang, M. Zhao, G. Liu, L. Dong, X. Liu, Alexandria Eng. J. **54**, 777–786 (2015)
4. Y. Li, Q. Du, T. Liu, X. Peng, J. Wang et al., Chem. Eng. Res. Des **91**, 361–368 (2013)
5. Y. Gokce, Z. Aktas, Appl. Surf. Sci. **313**, 352–359 (2014)
6. M. Ghaedi, A. Golestani Nasab, S. Khodadost, M. Rajabi, S. Azizian, J. Ind. Eng. Chem. **20**, 2317–2324 (2014)
7. N.R. Sirinivasan, P.A. Shankar, R. Bandyopadhyaya, Carbon. **57**, 1–10 (2013)
8. A. Bhatnagar, W. Hogland, M. Marques, M. Sillanpaa M, Chem. Eng. J. **219**, 499–511 (2013)
9. Y. Wang, GM. Xia, C. Wu, J. Sun, R. Song, W. Huang, Carbohydr. Polym. **115**, 686–693 (2015)
10. M. Auta, BH. Hameed, Colloid Surface B. **105**, 199–206 (2013)
11. A. Ghaee, M. Shariaty-Niassar, J. Barzin, A.F. Ismail, Int. J. Nanosci. Nanotechnol. **9**, 213–220 (2013)
12. S. Jiang, J. Lv, M. Ding, Y. Li, H. Wang, S. Jiang, Mater. Sci. Eng. C. **59**, 86–91 (2016)
13. NS. Prasad, S. Moulik, S. Bohra, KY. Rani, S. Sridhar, Carbohydr. Polym. **136**, 1170–1181 (2016)
14. NA. Reiad, OEA. Salam, EF. Abadir, FA. Harraz, J. Environ. Sci. **24**, 1425–1432 (2012)
15. S. Morelli, R.G. Holdich, M.M. Dragosavac, Chem. Eng. J. **288**, 451–460 (2016)
16. E. Salehi, S.S. Madaeni, L. Rajabi, V. Vatanpour, A.A. Derakhshan, S. Zinadini, S. Ghorabi, H. Ahmadi Monfared, Sep. Purif. Technol. **89**, 309–319 (2012)
17. Sh. Maghsoodloo, B. Noroozi, Ak. Hagi, G.A. Sorial, J. Hazard. Mater. **191**, 380–387 (2013)
18. Sh. Hydari, H. Shariffard, M. Nabavinia, M.R. Parvizi, Chem. Eng. J. **193–194**, 276–282 (2012)
19. SR. Sandeman, VM. Gunko, OM. Bakalinska, CA. Howell, Y. Zheng, MT. Kartel, GJ. Philips, SV. Mikhailovsky, J. Colloid Interface. Sci. **358**, 582–592 (2011).
20. J. Yang, K. Qiu, Chem. Eng. J. **166**, 209–217 (2010)
21. A. Rajeswari, A. Almalraj, A. Pius, J. Water Treat. Process. Eng. **9**, 123–134 (2016)
22. JE. Dos Santos, ER. Dockal, ETG. Cavalheiro, Carbohydr. Polym. **60**, 277–282 (2005)
23. RC. Bansal, M. Goyal, Activated Carbon Adsorption. Taylor & Francis group, Boca Raton (2005).
24. R. Aguliar, J. Nakamatsu, E. Ramirez, M. Elgegren, J. Ayarza, S. Kim, M.A. Pando, L. Ortega-San-Martin, Constr. Build. Mater. **114**, 625–637 (2016)
25. Y. Shi, D. Xiong, Y. Liu, N. Wang, X. Zhao, Mater. Sci. Eng. C. **65**, 172–180 (2016)
26. O. Farid, F. Mansour, M. Habib, J. Robinson, S. Tarleton, J. Environ. Chem. Eng. **4**, 293–298 (2016)